On the existence of bicontinuous cubic phases in dioleoylphosphatidylethanolamine

ARTICLE *in* BERICHTE DER BUNSENGESELLSCHAFT/PHYSICAL CHEMISTRY CHEMICAL PHYSICS · OCTOBER 1994

DOI: 10.1002/bbpc.19940981011

6 AUTHORS, INCLUDING:

Michael Rappolt
University of Leeds
117 PUBLICATIONS **2,641** CITATIONS

On the Existence of Bicontinuous Cubic Phases in Dioleoylphosphatidylethanolamine

J. Erbes, C. Czeslik, W. Hahn, and R. Winter

University of Dortmund, Institute of Physical Chemistry, Otto-Hahn-Straße 6, D-44221 Dortmund, Germany

M. Rappolt and G. Rapp

European Molecular Biology Laboratory (EMBL), Hamburg Outstation at DESY, D-22603 Hamburg, Germany

Key Words: Biophysical Chemistry / Cubic Phases / Membranes / Phase Transitions

Aqueous dispersions of 1,2-dioleoyl-sn-glycero-3-phosphatidylethanolamine (DOPE) exhibit a well-known phase transition from a lamellar liquid-crystalline (L_α) to an inverted hexagonal (H_{II}) phase as the temperature is raised above 13 °C. Recently, it has been reported [1, 2] that a bicontinuous cubic phase can be induced in this system, when the lipid is rapidly cycled between these two phases. Their X-ray diffraction results indicated that the cubic lattice is most consistent with either the Pn3m or Pn3 space group. In studies on similar systems [3, 4], two cubic phases could be detected in the L_α-H_{II} transition region, however. One aim of the present study was to investigate, if still further bicontinuous cubic phases can be induced in simple DOPE dispersions by changing the experimental conditions. Indeed, we found that two cubic lattices may be induced when the lipid system is cycled between −5 and 15 °C more than thousand times. The second goal of the present investigation was to study the temperature dependence of the lattice parameters, the stability and transformations of these cubic phases over a wide temperature range. It has been discussed that the presence of cubic phases may be a general feature of H_{II}-forming lipids in the region of their lamellar to hexagonal phase transition region and that non-lamellar lipid structures might play an important role as transient intermediates in biochemical processes.

Introduction

Aqueous dispersions of lipid bilayers, in particular the phosphatidylcholines and phosphatidylethanolamines, provide valuable models for the investigation of biophysical properties of membrane lipids [5, 6]. They exhibit a rich lyotropic and thermotropic phase behaviour. Most lipids in excess water exist in lamellar bilayer phases, although certain lipids can form a non-bilayer hexagonal (H_{II}) or cubic liquid-crystalline phases as well [5 – 15]. Fig. 1 gives examples of the structure of different lipid phases.

Many naturally derived lipids, such as phosphatidylethanolamines, phosphatidic acid, phosphatidylglycerol, cardiolipin and monoacylglycerides, can form or induce the formation of a hexagonal phase. The H_{II} phase is an inverted hexagonal phase with the polar head groups lining the inside of long cylinders and the hydrocarbon tails facing outwards.

Many of the cubic liquid-crystalline phases are now known to consist of bicontinuous regions of water and hydrocarbon. Two examples are given in Fig. 1c. Bicontinuous cubic phases can be described by periodic minimal surfaces, which are well known in differential geometry [16]. In the case of inverted bicontinuous cubic phases, the periodic minimal surfaces lie along the middle of the bilayer. Such surfaces are saddle surfaces and have the property that their mean curvature is zero everywhere and that their Gaussian curvature is negative [7, 8, 12]. These periodic minimal surfaces are connected by a Bonnet transformation, which occurs in a way as to leave the Gaussian curvature at all points unchanged, and to preserve all angles, distances and areas on the surface. The two head group surfaces of the lipid bilayer do not, in general, have zero mean curvature, however.

It is assumed that non-lamellar lipid structures are also of great biological relevance and that they are more common than was previously realized [6, 7, 10, 12, 17]. These non-lamellar phases, which occur for a number of membrane lipids probably play an important functional role in some cell processes as local and transient intermediates. For example, cubic phases seem to be more or less directly involved in membrane fusion, fat digestion, and the reorganization of cell membrane composition. There is also evidence that microorganisms control the lipid composition of their membranes so as to maintain them close to a composition where non-lamellar structures would begin to appear [18, 19], which could rather easily be induced by small perturbations in physiologial ionic strength, pH etc. It has been observed that Acholeplasma Laidlawii A, a bacterial organism that is deficient in fatty acid synthesis, selects among fed fatty acids in such a way as to maintain the non-lamellar transition temperature of its membrane only several degrees above the growth temperature. Gruner et al. [10, 11] suggested that the membrane tries to maintain a constant spontaneous curvature at the growth temperature.

Recently, it has been reported [1, 2] that an inverted cubic phase with space group Pn3m or Pn3 can be induced in 1,2-dioleoyl-sn-glycero-3-phosphatidylethanolamine (DOPE)-water dispersions between the lamellar liquid-crystalline and the inverted hexagonal phase, when the lipid is rapidly cycled between these two phases hundreds of times. The occurrence of more than one cubic structure might be possible, however, as a transformation between bicontinuous cubic phases is possible without changing the curvature-free energy of the lipid bilayer [20 – 22]. One aim of the present study was to investigate, if still further cubic phases can be induced in DOPE dispersions by changing the experimental conditions. A further aim was to study the

  0005-9021/94/1010-1287 $ 10.00+.25/0

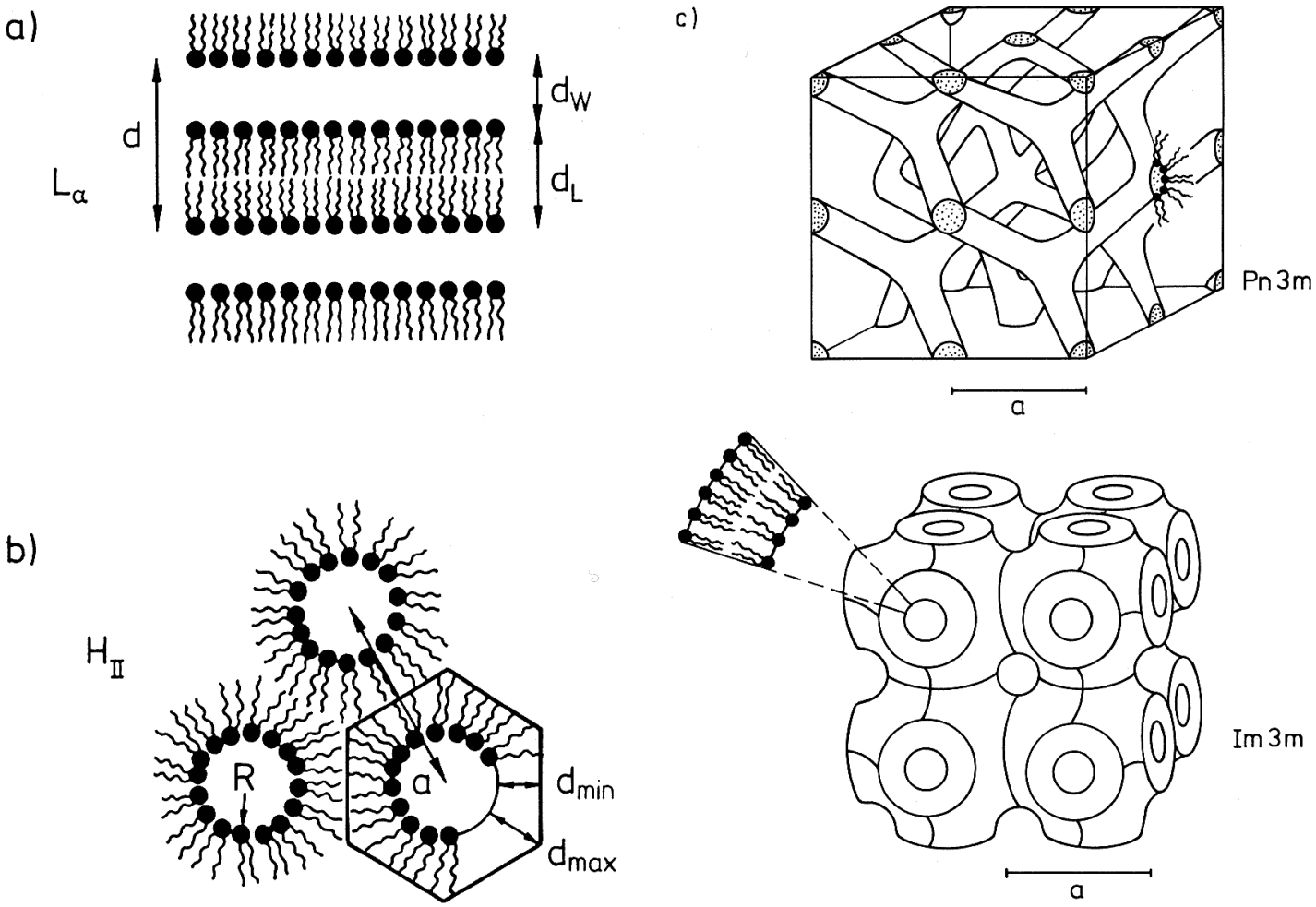

Fig. 1
Schematic drawing a) of a multilamellar liquid-crystalline (L_α) bilayer, consisting of a one dimensional stacking of amphiphilic bilayers, with lamellar repeat unit d, b) of the inverted hexagonal (H_{II}) phase with negative mean interfacial curvature. The average thickness of the hydrocarbon layer is seen to lie between d_{min} and d_{max} around a cylindrical water core of radius R, illustrating the problem of filling the hydrocarbon volume of the phase with lipid chains in the interstitial chain region, and c) of the double diamond cubic liquid-crystalline phase Pn3m with D minimal surface and the "plumber's nightmare" cubic phase Im3m based on Schwarz's P minimal surface

temperature dependence of the lattice parameters of the different cubic lipid phases and their stability over a wide temperature range, in order to explore the geometrical and epitaxial relations which exist between different coexisting phases. For these reasons, a thermal cycling process was developed to induce different metastable cubic phases in this system. Such studies should be also useful in analysing the underlying mechanisms of lipid phase transitions.

In order to characterize the temperature-dependent structure of the sample, we applied the X-ray diffraction technique using synchrotron radiation. In addition to the X-ray studies, ^{31}P NMR and differential scanning calorimetry (DSC) were used to characterize the samples and their temperature-dependent phase behaviour.

Experimental

DOPE (1,2-dioleoyl-sn-glycero-3-phosphatidylethanolamine) was obtained from Avanti (Birmingham, Alabama, USA) and was used without further treatment. Aqueous dispersions of 30 – 50 wt.% lipid were prepared by weighing the appropriate amounts of lipid and bidistilled water, and a homogeneous dispersion was obtained after five freeze-thaw-vortex-cycles. The vortexing of the sample was performed at a temperature above the gel to liquid-crystalline phase transition temperature of the lipid system ($T_m \approx -6\,°C$).

The calorimetric measurements were performed on a Perkin-Elmer DSC7 differential scanning calorimeter (DSC). The lipid mixture was filled into stainless steal pans, which were then sealed in a press. DSC scans were taken after overnight equilibration at 0 – 4 °C. The sample was heated together with a blank at a programmed heating rate of 2 °C/min. To evaluate the phase transition temperatures, a straight line was fitted to the upward deflection of the DSC transition curve. The enthalpies of transitions were evaluated from the areas under the calorimetric curves.

The small-angle X-ray diffraction experiments were performed at beam line X13 of the EMBL outstation at DESY (storage ring DORIS, 4.5 GeV, 20 – 60 mA). Beam line X13 comprises of a monochromator-mirror arrangement [23] with a triangular germanium monochromator for horizontal focusing and 12 plane quartz mirrors aligned on an aluminium bench for vertical focusing. With the mono-

chromator used, the wavelength of the X-rays was 1.5 Å, higher harmonics were rejected by the mirrors. Sets of tungsten slits were used to adjust the beam size at the sample (approx. 0.5 mm in height and 4 mm in width) and to reduce parasitic scattering. One-dimensional diffraction patterns were recorded using a sealed linear detector with delayline readout [24] as part of the standard data acquisition system [25], which was controlled by a PC. Excess radiation was avoided with a small selenoid driven shutter close to the sample. Additional information, like temperature, ring current and X-ray flux measured with an ionisation chamber in front of the sample, was stored on the local memory. Data were normalized for the ionisation chamber and were analysed using the interactive data evaluation programme OTOKO [26]. The distance between sample and detector was 175 cm. The samples of 100 µl volume were contained between two 25 µm thick mica windows, which were held in a thermostatically controlled steal holder. The reciprocal spacings $s = 1/d = (2/\lambda)\sin\theta$ (d: reciprocal lattice spacing, 2θ: scattering angle, λ: wavelength of radiation) were calibrated by the diffraction pattern of rat-tail collagen with a long spacing of 640 Å.

^{31}P NMR spectra were obtained by using a Bruker 400 spectrometer operating at 162 MHz for ^{31}P. The thermally cycled samples were placed in 10 mm NMR tubes, and 1 ml of D_2O was added for the purpose of maintaining deuterium lock. Spectra were accumulated for up to 8000 transients in the presence of high-power broad-band proton decoupling.

Experimental Results and Discussion

DOPE-water dispersions readily undergo a lamellar L_β to liquid-crystalline L_α transition at $T_m = -6\,°C$. Increase in temperature generally results in an increased configurational disorder from the head group towards the end of the hydrocarbon chains, which results in a tendency for forming a wedge-shape of the lipid molecule and finally leads to a temperature-induced lamellar to inverted hexagonal H_{II} phase transition. The curved interface of a H_{II} phase allows the chains to splay more apart while allowing the interfacial area to keep small (see Fig. 1 b).

In rather good agreement with previously published data [27 – 29], we found in our DSC studies of a 30 wt.% DOPE dispersion a transition temperature T_h for the L_α-H_{II} conversion of about 13 °C, as can be inferred from Fig. 2. The sample was preincubated over night at 0 °C before the DSC run. Whereas the main transition of DOPE-water is accompanied by an enthalpy change ΔH_m of about 20 kJ/mol [27, 28], from the DSC scan of Fig. 2 a value for the lamellar-hexagonal transition enthalpy change ΔH_h of only 2 kJ/mol can be evaluated. The corresponding transition entropy of the latter transition is 7 $Jmol^{-1}K^{-1}$. In view of the large topological structural changes that have to take place during the L_α-H_{II} transition, it is surprising that the transition enthalpy is significantly lower than that of the gel to liquid-crystalline transition. However, since the lamellar to non-lamellar transition takes place wholly in a fluid-like

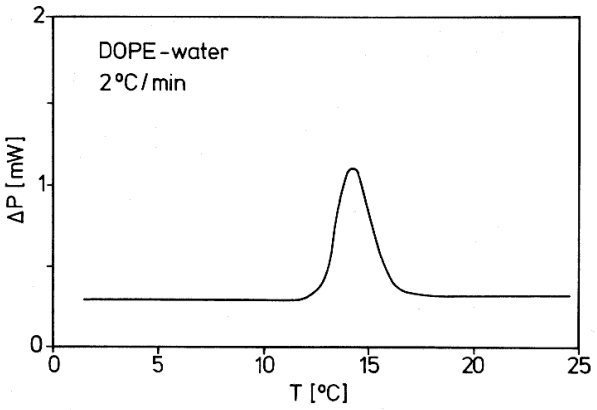

Fig. 2
DSC trace of a 30 wt.% DOPE-water dispersion (heating scan rate: 2 °C/min)

state, both the transition enthalpy and transition entropy are relatively small compared to those of the main chain-melting transition.

Fig. 3 exhibits the temperature-dependent X-ray diffraction data of a 30 wt.% DOPE-water dispersion in the temperature range from 10 to 18 °C. The scan rate was 2 °C/min and the time for taking one X-ray diffraction pattern took 5 s. Clearly, the lamellar L_α to hexagonal transition is visible around 13 °C by a drastic change in the diffraction pattern. Below 13 °C, the first lamellar diffraction peak with interlamellar repeat distance d of 51 Å is seen, which is in good agreement with the value of 52 Å, which has been found for the L_α-repeat distance at 2 °C [1]. d consists of the lipid bilayer thickness d_L including the interlamellar water layer distance d_w (see Fig. 1 a). Above the lamellar to hexagonal lipid phase transition, the pattern indicative of a hexagonal lattice (peaks spaced in the ratio $1:\sqrt{3}:2:\sqrt{7}:\ldots$) is seen. The three Bragg peaks observed correspond to the (10), (11) and (20) reflections of the H_{II} structure. No intermediate phases appear in course of the phase transition, i.e. the L_α-H_{II} transition proceeds as a two state process at these experimental conditions. The lattice constant a of the hexagonal phase (center-to-center distance of adjacent cylinders – see Fig. 1 b), which has been

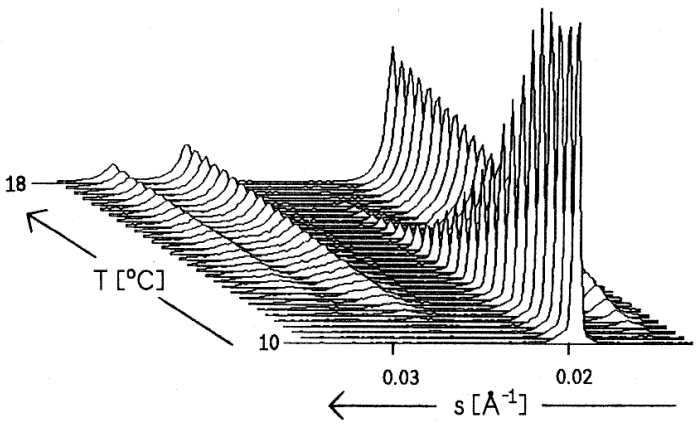

Fig. 3
X-ray small-angle diffraction pattern of a 30 wt.% DOPE dispersion during a heating experiment with 2 °C/min. The exposure time was 5 s/frame

calculated from $1/s = (2/a\sqrt{3})(h^2+k^2+hk)^{1/2}$ (h, k: Miller indices), is 75 Å at 15 °C and decreases with about −0.2 Å/°C with increasing temperature. Interestingly, similar lattice parameters of about 50 Å for the L_α phase and of about 78 Å for the H_{II} phase have been observed close to T_h for phosphatidylethanolamine systems of similar effective chain length [30], which reflects the fact that the hydrocarbon packing sets the maximum size of the H_{II} lattice.

It has been shown by Gruner et al. [1, 2], that in DOPE also a cubic primitive structure can be induced by subjecting the sample to an extensive temperature cycling process between −5 to 15 °C, i.e. at temperatures close to the L_α-H_{II} transition region. Following their procedure, we built a computer-controlled cycling system, which allows a large amount of sample (ca. 500 − 1000 mg) to be automatically thermalized hundreds of times between these two temperatures. The waiting time at each temperature was chosen to be 2 min. The final cycled specimen after 1400 cycles looked like a highly viscous translucent gel. Thin-layer chromatography on the cycled samples did not show any sign of lipid degradation during the cycling process. Interestingly, the sample can be reset by cooling it down to temperatures below −6 °C. The sample then exhibits the equilibrium L_α-H_{II} transition at 13 °C, again. DSC studies on the cycled samples revealed DSC peaks at a temperature that is similar to T_h of the uncycled DOPE dispersion, the enthalpy change has diminished, however. It decreases from 2 to about 1 kJ/mol after e.g. 500 temperature cycles.

Fig. 4 shows the results of ^{31}P NMR measurements of hydrated 50 wt.% DOPE at 2 °C that was thermally cycled 500 times. For comparison, the ^{31}P NMR spectra of DOPE dispersions in their liquid-crystalline and inverted hexagonal state are given. The lamellar phase gives rise to a broad spectrum with a high-field peak and a low-field shoulder, i.e., a negative chemical shift anisotropy. The inverted hexagonal phase generates a phosphorous NMR spectrum with a low-field peak and a high-field shoulder, i.e., a positive chemical shift anisotropy. The magnitude of its chemical shift anisotropy is reduced by a factor of two

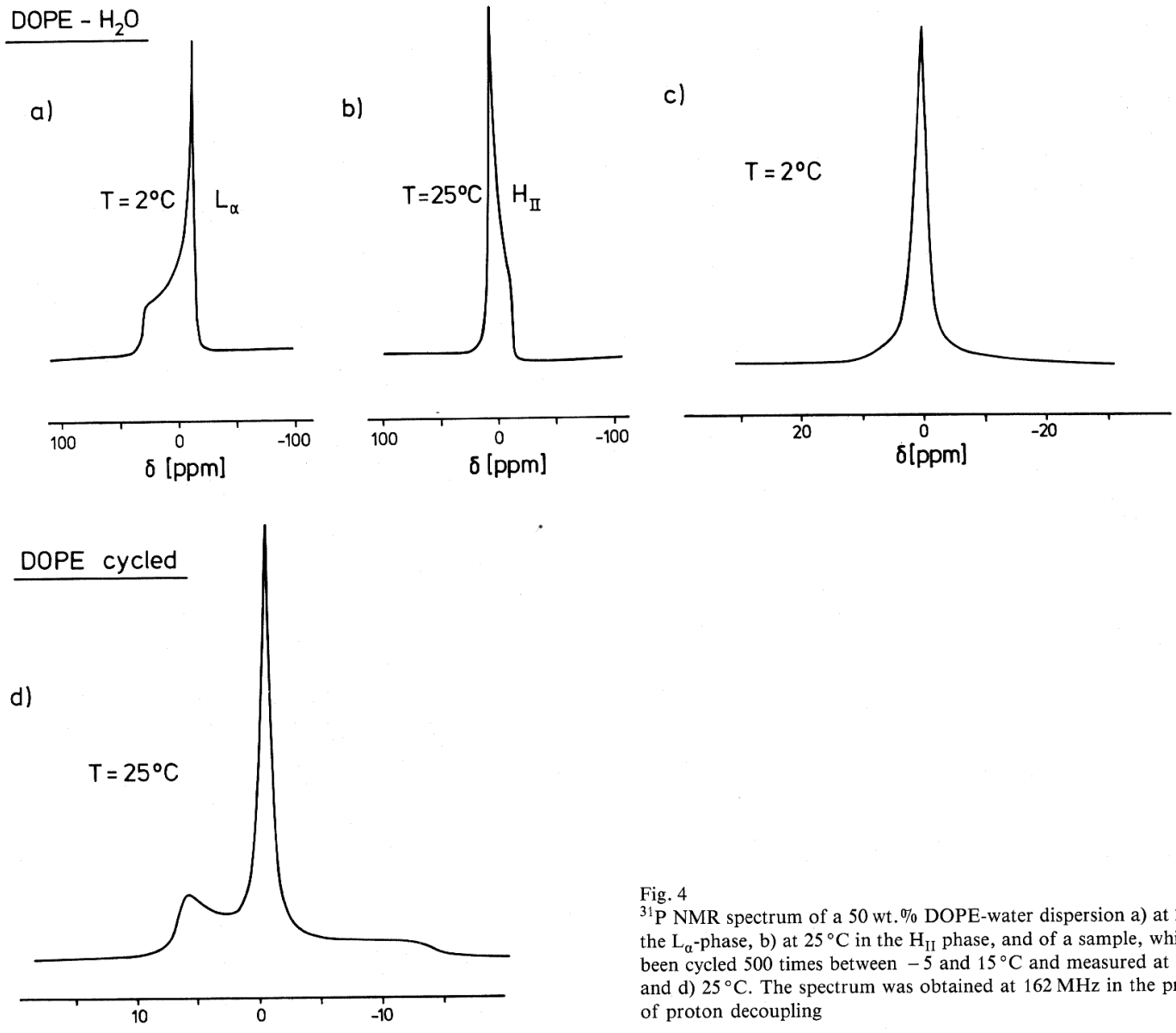

Fig. 4
^{31}P NMR spectrum of a 50 wt.% DOPE-water dispersion a) at 2 °C in the L_α-phase, b) at 25 °C in the H_{II} phase, and of a sample, which has been cycled 500 times between −5 and 15 °C and measured at c) 2 °C and d) 25 °C. The spectrum was obtained at 162 MHz in the presence of proton decoupling

as compared to the spectrum from the lamellar phase [31, 32]. As can be clearly seen in Fig. 4, the spectrum of the cycled sample at 2 °C, however, reveals a narrow isotropic resonance of full width at half height of about 200 Hz, similar to that reported for other phospholipids in their cubic phases [7, 12]. In addition, Fig. 4 includes an example of a phosphorous NMR spectrum of that sample at a higher temperature. At 25 °C, the ^{31}P NMR signal has broadened, and one can see that the sample has been partially transformed into the inverted hexagonal phase. The existence of narrow ^{31}P signals, which are indicative of the existence of cubic phases, has been observed for DOPE-water dispersions over a concentration range from 50 to 60 wt.% water.

Fig. 5 shows the X-ray diffraction pattern of a sample cycled 1400 times and measured at 5 °C. The peaks show index as two cubic lattices. One of them consists of four orders of diffraction space in the ratio $\sqrt{2}:\sqrt{3}:\sqrt{6}:\sqrt{9}$. A unit cell space group consistent with orders spaced in these ratios is Pn3m with a 132 Å unit cell. Three orders spaced in the ratio $\sqrt{2}:\sqrt{4}:\sqrt{6}$ were observed for the second lattice, which can be assigned to a body-centered lattice of the Im3m space group with a unit cell length of 168 Å. A definite lattice assignment on so few orders of reflection is not possible, however. A metric relation of about 1.27 between the repeat units of the two cubic lattices has been found in other lipid systems, too [20–22].

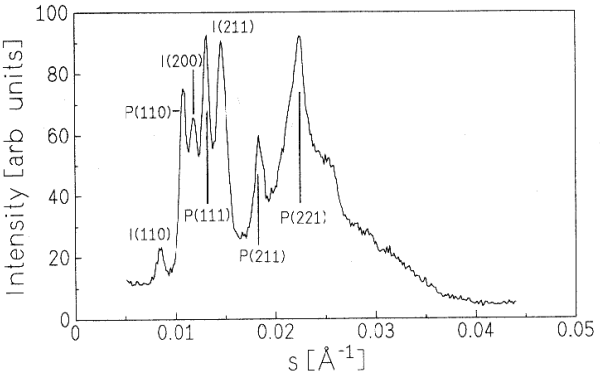

Fig. 5
X-ray small-angle diffraction pattern of a 50 wt.% DOPE-water dispersion at $T = 5$ °C, which has been cycled 1400 times across the L_α-H_{II} transition, and indexing of the diffraction patterns: I(*hkl*): body-centered cubic phase Im3m, P(*hkl*): cubic primitive phase Pn3m

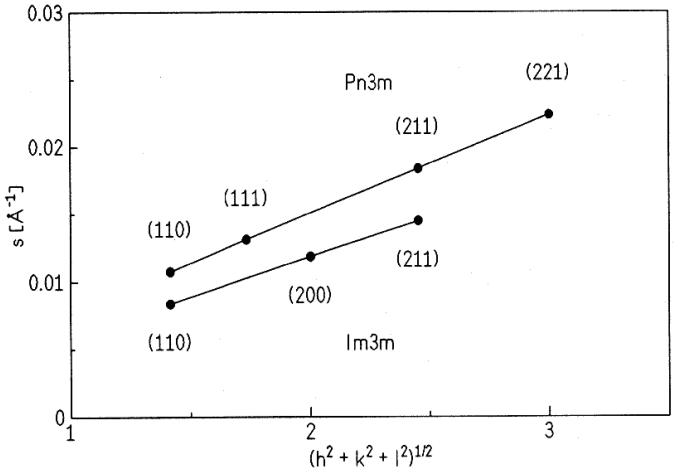

Fig. 6
Reflex positions for the two cubic lattices vs. $(h^2+k^2+l^2)^{1/2}$. The spacing between the lines fall in the ratios as would be expected for a Pn3m and an Im3m cubic space group, respectively. The lattice parameters are given by the reciprocal gradients of the plots

The reflex positions of the peaks of the two lattices are shown in Fig. 6 plotted vs. $(h^2+k^2+l^2)^{1/2}$ for the *hkl* indices. All points from each lattice should fall on a straight line whose slope is used to determine the dimensions of the unit cell.

Fig. 7 displays a selection of diffraction patterns of a 50 wt.% DOPE dispersion, which has been cycled between the L_α and H_{II} transition 1400 times, as a function of temperature, ranging from 4 up to 78 °C. The scan rate was 0.5 °C/min, the X-ray exposure time was 5 s/frame. Clear-

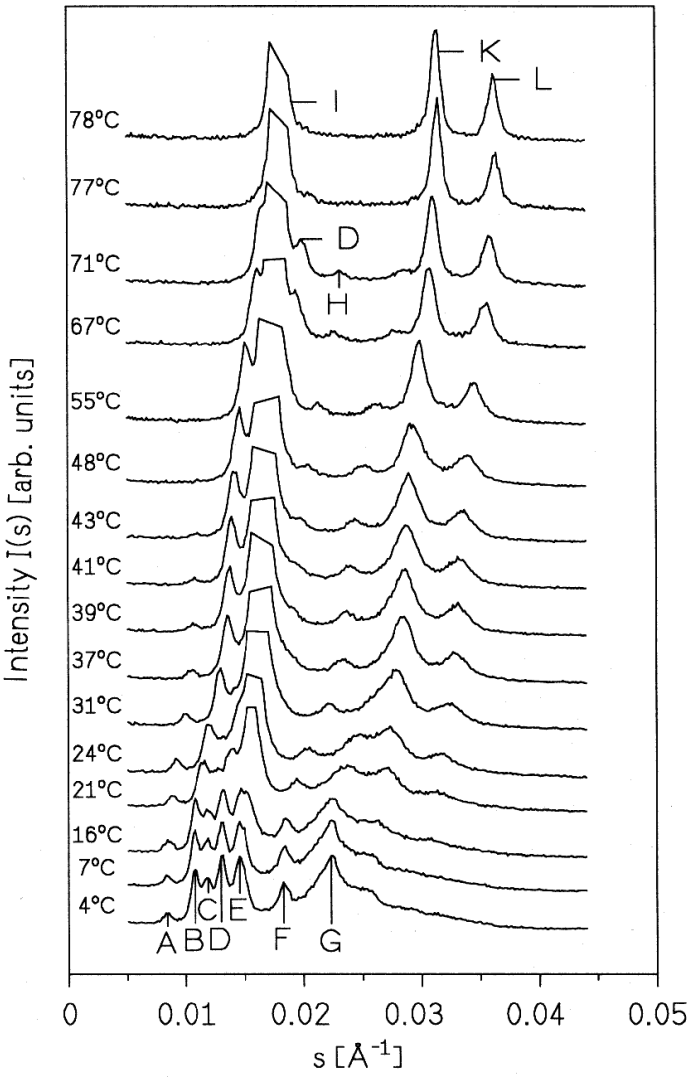

Fig. 7
Selection of X-ray small-angle diffraction patterns of a 50 wt.% DOPE dispersion, which has been cycled between the L_α and H_{II} transition 1400 times, during a heating experiment with 0.5 °C/min. The X-ray exposure time was 5 s/frame. The indexing (*hkl*) of the diffraction patterns is: A: I(110), B: P(110), C: I(200), D: P(111), E: I(211), F: P(211), G: P(221), H: P(200), I: hexagonal (10), K: hexagonal (11), L: hexagonal (20). I(*hkl*): body-centered cubic phase Im3m, P(*hkl*): cubic primitive phase Pn3m. The (10) reflex notation I of the hexagonal phase has been cut off

ly, a series of temperature-dependent structural changes are visible. The broad incoherent scattering background lying underneath the Bragg reflections indicates that part of the specimen is not well ordered. The indices of the reflex positions A – L of the different structures are given in the figure caption. Fig. 8 exhibits the reflex positions of the different phases as a function of temperature. The cubic phase Im3m disappears at about 45 °C, whereas the cubic primitive phase is stable up to about 75 °C. No direct interconversion of the cubic structures has been observed. Above about 13 °C, the inverted hexagonal H_{II} phase is forming, in agreement with the DSC results. The Bragg reflections (10), (11) and (20) of the hexagonal phase are formed out of the structureless diffusive scattering background. Their intensities drastically increase up to about 30 °C. Above that temperature, the intensity is still slowly progressing, possibly due to the transformation of the cubic phases into the H_{II} phase, which is indicated by the gradual diminuation in intensity of the reflections of the two cubic lattices above about 30 °C.

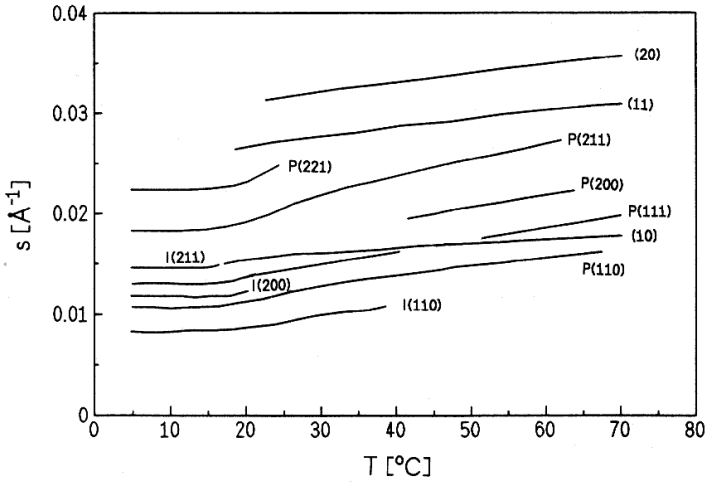

Fig. 8
Reflex positions of a 50 wt.% DOPE dispersion, which has been cycled between the L_α and H_{II} transition 1400 times, as a function of temperature

Fig. 9 shows the lattice parameters of the three non-lamellar phases as a function of temperature. Interestingly, the lattice constants of the cubic phases are constant up to about 15 °C $\approx T_h$, they start to decrease non-linearly above that temperature, however. At e.g. 20 °C, three lattices coexist: the cubic phases Pn3m and Im3m with lattice constants 128 Å and 162 Å, respectively, and the hexagonal phase with a lattice spacing of 76 Å. At 25 °C, the temperature dependence of the Pn3m cubic lattice parameter a is found to be -1.8 Å/°C and $(da/dT)_p$ is about -0.4 Å/°C at 60 °C.

We note that similar experiments were performed on N-methylated DOPE (DOPE-Me) [3]. Also in this system, the formation of two cubic phases with space groups Pn3m or Pn3 and Im3m has been observed in the region between the lamellar and inverted hexagonal phase. For DOPE-Me, cooling from the H_{II} phase to room temperature and then

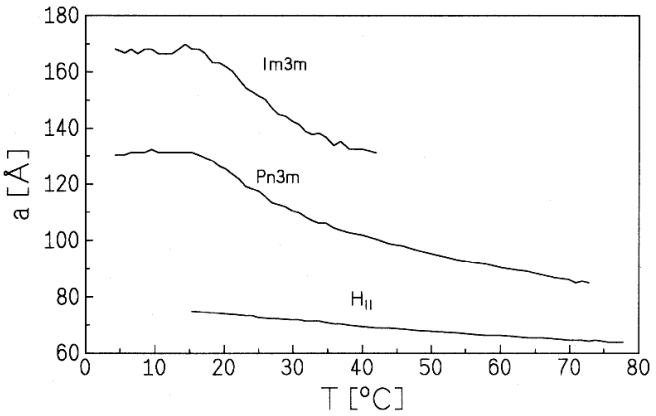

Fig. 9
Lattice constants a of the inverted hexagonal phase and the two cubic phases Pn3m and Im3m of the cycled 50 wt.% DOPE dispersion as a function of temperature

storing for months, led to the formation of two coexisting cubic phases, of probable space groups Pn3m with $a = 136$ Å and Im3m with $a = 175$ Å, respectively. The ratio of the lattice parameters of the two cubic phases is similar to that found in our cycled DOPE dispersions.

As can be deduced from these investigations, the formation and occurrence of DOPE cubic phases is sensitive to the thermal history of the sample, such as the rate and number of thermal cycling processes across the L_α-H_{II} transition. Siegel [31 – 35] has suggested that the formation of these cubic structures may arise from topological defects, such as inverted micellar intermediates and interlamellar attachments, of the membrane surface that are generated by cycling through the L_α-H_{II} transition. One might speculate that the number of these lipid-water interface defects increases as one repeatedly crosses the L_α-H_{II} transition, as long as the temperature change is not so extreme as to anneal out these created defects. Eventually, these topological defects coalesce to form a new lattice that is due to a bicontinuous cubic structure.

A molecular level understanding of the phase behaviour of these lipid systems would require a detailed consideration of many interactions. This lies beyond the present understanding of these complex systems, however. Nevertheless, some qualitative arguments can be given [5, 7, 8, 11 – 15]. The non-lamellar phases have curved lipid-water interfaces. Generally, a lipid layer will tend to curl if doing so relieves stress within the layer which may arise from an asymmetry in the lateral interactions within the head groups as compared to the hydrocarbon regions. For example, the lipid bilayer has a greater tendency to curl if the splay of hydrocarbon chains increases at higher temperatures. In the model of Kirk et al. [14] for the L_α-H_{II} transition, four important contributions to the free energy of the lipid system are considered: a curvature free energy associated with bending of the monolayers, a cost in free energy to the packing of hydrocarbon chains in an eventually non-homogeneous environment, a hydration repulsion term due to surface polarization effects, and a free energy term due to electrostatic interactions. The curvature free energy quantifies the tendency of the layer to curl. Thus, in general, a

free lipid monolayer will prefer to have a certain spontaneous radius of curvature R_0, and any deviations from this radius of curvature will result in an increase in free energy. R_0 is determined by imbalances of the lateral stresses in the lipid monolayer, such as the repulsive lateral pressure in the chain region due to thermally excited cis-trans rotations of the hydrocarbon chains, the hydrophobic effect which results in an interfacial tension, which acts to minimize the hydrocarbon-water interfacial area, and the lateral stress around the lipid head groups, being due to steric, hydrational, electrostatic and hydrogen bonding interactions. If, for example, the chain pressure is dominant at higher temperatures, the monolayer will curl towards the aqueous region. In the lamellar bilayer state, this desire for monolayer curvature is physically frustrated, however, because energetically expensive voids would be formed in the core of the bilayer. This inability of a system to satisfy simultaneously the condition of uniform curvature and optimal packing has been termed a state of frustration. There are only a few ways in which the system can relieve this frustration, e.g. by a topological phase transformation. R_0 is strongly effected by temperature. Increasing temperature decreases R_0, which would favour a hexagonal structure. Competing against the curvature energy is the free energy cost to pack efficiently the hydrocarbon chains within a H_{II} unit cell (see Fig. 1 b). The packing free energy in the L_α phase is smaller since here the hydrocarbon chain thickness is uniform. At some temperature, however, the curvature constraint becomes too large and the transition to the hexagonal phase occurs. The repeat spacing $a(T)$ of the inverted hexagonal structure has been shown to decrease with increasing temperature, which is essentially a consequence of the growing disorder within the chains, resulting in a smaller radius R of the water core.

In the H_{II} phase, for which $R \approx R_0$, the curvature energy is low but the chain packing energy can be considerable. Since the phase behaviour is governed by the sum of both contributions, it is possible for either the L_α or H_{II} phase to have an overall lower free energy. Andersson et al. [20] showed that, in certain situations, the topology of bicontinuous cubic phases can result in less frustration and hence a lower free energy than either the lamellar or H_{II} phase. The bicontinuous cubic phases do not suffer the extreme chain packing stress of the H_{II} phase, their geometry does not fully avoid physical frustration, however. It has been suggested [10, 11, 15] that small values of R_0 lipid systems exhibit low-temperature L_α-H_{II} transitions, intermediate R_0 systems exhibit complex non-equilibrium transition behaviour and are likely to form cubic phases, and large R_0 systems are stable as L_α-phases. This might lead to the suggestion, that cubic states may be universal features of lipid systems with intermediate spontaneous curvature, that normally exhibit inverted H_{II}-phases. The underlying universality of this phase behaviour may be obscured by large kinetic barriers, however.

We are grateful to the Deutsche Forschungsgemeinschaft and the Fonds der Chemischen Industrie for financial support.

References

[1] E. Shyamsunder, S.M. Gruner, M.W. Tate, D.C. Turner, P.T.C. So, and C.P.S. Tilcock, Biochemistry *27*, 2332 (1988).
[2] P.T.C. So, S.M. Gruner, and S. Erramilli, Phys. Rev. Lett. *70*, 3455 (1993).
[3] S.M. Gruner, M.W. Tate, G.L. Kirk, P.T.C. So, D.C. Turner, and D.T. Keane, Biochemistry *27*, 2853 (1988).
[4] J.M. Seddon, J.L. Hegan, N.A. Warrender, and E. Pebay-Peyroula, Progr. Colloid Polym. Sci. *81*, 189 (1990).
[5] G. Cevc and D. Marsh, Phospholipid Bilayers, John Wiley & Sons, New York 1987.
[6] P. Yeagle, The Structure of Biological Membranes, CRC Press, Boca Raton, Florida 1992.
[7] J.M. Seddon, Biochim. Biophys. Acta *1031*, 1 (1990).
[8] J.M. Seddon and R.H. Templer, Phil. Trans. R. Soc. Lond. A *344*, 377 (1993).
[9] D. Marsh, Chem. Phys. Lipids *57*, 109 (1991).
[10] S.M. Gruner, Ann. Rev. Biophys. Chem. *14*, 211 (1985).
[11] M.W. Tate, E.F. Eikenberry, D.C. Turner, E. Shyamsunder, and S.M. Gruner, Chem. Phys. Lipids *57*, 147 (1991).
[12] G. Lindblom and L. Rilfors, Biochim. Biophys. Acta *988*, 221 (1989).
[13] M. Caffrey, Biochemistry *24*, 4826 (1985).
[14] G.L. Kirk, S.M. Gruner, and D.L. Stein, Biochemistry *23*, 1093 (1984).
[15] S.M. Gruner, J. Phys. Chem. *93*, 7562 (1989).
[16] H.A. Schwarz, Monatsber. Dtsch. Akad. Wiss. Berlin 149 (1865).
[17] P. Mariani, V. Luzzati, and H. Delacroix, J. Mol. Biol. *204*, 165 (1988).
[18] J.E. Cronan and P.R. Vagelos, Biochim. Biophys. Acta *265*, 25 (1975).
[19] L. Rilfors, A. Wieslander, and S. Stahl, J. Bacteriol. *135*, 1043 (1978).
[20] S. Andersson, S.T. Hyde, K. Larsson, and S. Lidin, Chem. Rev. *88*, 221 (1988).
[21] D.M. Anderson, S.M. Gruner, and S. Leibler, Proc. Natl. Acad. Sci. USA *85*, 5364 (1988).
[22] S.T. Hyde and S. Andersson, Z. Kristallogr. *168*, 213 (1984).
[23] J. Hendrix, M.H.J. Koch, and J. Bordas, J. Appl. Cryst. *12*, 467 (1979).
[24] A. Gabriel and F. Dauvergne, Nucl. Instrum. Meth. *201*, 223 (1982).
[25] C.J. Boulin, R. Kempf, A. Gabriel, and M.H.J. Koch, Nucl. Instrum. Meth. A *269*, 313 (1988).
[26] C. Boulin, R. Kempf, M.H.J. Koch, and S.M. McLaughlin, Nucl. Instrum. Meth. A *249*, 399 (1986).
[27] P. Cullis, P. Van Dijck, B. de Kruiff, and J. De Gier, Biochim. Biophys. Acta *513*, 21 (1978).
[28] P. Van Dijck, Biochim. Biophys. Acta *555*, 89 (1979).
[29] W. Hahn, Diploma-Thesis, University of Marburg (1993).
[30] R.N.A.H. Lewis, D.A. Mannock, and R.N. McElhaney, Biochemistry *28*, 541 (1989).
[31] P.L. Yeagle, in: "Biological Magnetic Resonance" Vol. 8, pp. 1–54, L.J. Berliner and J. Reuben (Eds.), Plenum Press, New York 1990.
[32] J. Seelig, Biochim. Biophys. Acta *515*, 105 (1978).
[33] D. Siegel, Biophys. J. *49*, 1155 (1986).
[34] D. Siegel, Biophys. J. *49*, 1171 (1986).
[35] D. Siegel, Chem. Phys. Lipids *42*, 279 (1986).

(Received: May 16, 1994
final version: July 4, 1994) E 8686